Spectral recovery from natural scenes with an RGB digital camera

Eva M. Valero, Juan L. Nieves
Departamento de Óptica, Fac. de Ciencias, Universidad de Granada, 18071-Granada (SPAIN)

Sérgio M. C. Nascimento
Department of Physics, Minho University, Campus de Gualtar, 4710-057 Braga, (Portugal)

Kinjiro Amano and David H. Foster
Computational Neuroscience Group, Faculty of Life Sciences, Moffat Building, University of Manchester, Manchester M60 1QD (UK)

Abstract

Multispectral images of natural scenes have been used to obtain a recovery matrix that transforms directly R, G, B values to spectral radiance without using linear models for spectral reflectances and illuminants. The R, G, B are simulated digital counts from a standard CCD camera. This recovery method had not been tested in natural scenes with uncontrolled illumination and for spectral radiance. We have used three different test data sets to check the method's accuracy, and three different quality measures to test the similarity between recovered and original spectral radiances (Goodnes-of-Fit, Root-Mean-Square-Error and ΔE^*_{ab} *colour difference). With this simple colorimetric system it was found that natural spectra could be recovered with a quality that is adequate for many applications.*

Introduction

Multispectral imaging attempts to recover radiance or reflectance spectra at each point of a scene of interest from limited spectral data [1],[2]. Typically, a multispectral system consists of a digital camera coupled to a range of spectrally broad-band filters. If the number of filters is sufficiently large and their bandwidths are sufficiently small, as with a hyperspectral imaging system [3], spectral data can be recovered exactly [3],[4]. But with just a few broad-band filters, or in the limit with the three native sensors of an RGB camera, spectral recovery presents an ill-posed problem.

Many multispectral-imaging methods exploit the underlying smoothness of signal spectra [5], with illuminants [6] and spectral reflectances [7] represented by low-dimensional models. If the number of coefficients is more than the number of camera-response values, then the latter may need to be effectively increased by introducing coloured filters or by imaging the scene under different illuminants [8], in order to achieve the same numbers of responses and coefficients.

Instead of using low dimensional models, however, the set of signal spectra may be estimated directly from the set of camera responses**.** This "direct-mapping" method has been applied successfully in specific conditions such as illuminant estimation [2] and spectral analysis of artworks [8]. But it is not clear whether the technique is efficient for natural spectra, particularly in conditions where the illumination is uncontrolled, as with natural scenes.

The aim of the present work was to estimate computationally the quality of spectral recovery of natural radiances based on a direct-mapping method, in which the only information available was from the three RGB sensors. The natural radiance spectra were taken from a hyperspectral database. With this simple system it was found that spectra could be recovered sufficiently accurately for many practical applications.

Methods

Hyperspectral data from thirty scenes, fifteen from rural and fifteen urban environments, were selected from a high-spatial-resolution database [9]. The data were obtained with a Peltier-cooled digital monochromatic camera with spatial resolution 1344 × 1024 pixels (Hamamatsu, model C4742-95-12ER, Hamamatsu Photonics K.K., Japan) with a fast-tunable liquid-crystal filter (VariSpec, model VS-VIS2-10HC-35-SQ, Cambridge Research & Instrumentation, Inc., MA, USA) mounted in front of the lens, with infra-red blocking filter. Spectral radiances at each pixel element were obtained. The accuracy checking procedure was done by the use of a telespectroradiometer (SpectraColorimeter, PR-650, PhotoResearch Inc., Chatsworth, Calif.), whose calibration was traceable to the National Physical Laboratory.

The RGB digital camera whose spectral sensitivities were used to compute the camera responses had spatial resolution 1280 × 1024 pixels (QImaging, model Retiga 1300, QImaging Corp., Canada) and 12 bits intensity resolution per channel. Several scene fragments were used for the training and test sets. The "matrix-training set", used to obtain the recovery matrix, was formed from 30 different fragments taken from the 30 scenes, each fragment of size 151 × 151 pixels. Each radiance spectra was defined over 400-700 nm in 10 nm intervals. These spectra were interpolated at 5-nm intervals to match the sampling interval for the camera spectral sensitivities, so each radiance spectra had 61 spectral values corresponding to different wavelengths.. The total number of spectral radiances in this matrix-training set was 684030. The influence of any possible correlation between adjacent pixels was tested for by sampling half of the scenes over alternate pixels vertically and horizontally (i.e. every fourth pixel) and comparing the recovered radiance spectra with those obtained from the unsampled scenes. The two sets of recovered signals (whose distributions were non-normal by the Kolmogorov-Smirnov test) were significantly different for all filter combinations ($p < 0.001$, Wilcoxon signed rank test).

The camera responses h_i to these spectra (i = 1, 2, 3 for red, green, and blue sensors, respectively) were computed as follows. At each pixel, suppose that S(λ) is the signal spectrum; Ri(λ) is the camera spectral sensitivity for each sensor i, where λ = 400, 405, …, 700 nm. Then

$$h_i = \sum_{\lambda=400}^{700} S(\lambda) R_i(\lambda) \qquad (1)$$

The computed camera responses were combined to form the response matrix **H** for the entire radiance set. The matrix **H** had then dimensions 3 x 684030. The matrix training set formed the **S** matrix of spectral radiances, of size 684030x61. The recovery matrix **D** was then computed from the pseudoinverse $\mathbf{H}^+$ of **H** by

$$\mathbf{D} = \mathbf{S}\mathbf{H}^+ . \qquad (2)$$

If **H** has full rank, then $\mathbf{H}^+ = (\mathbf{H}^t\ \mathbf{H})^{-1}\ \mathbf{H}^t$, where $\mathbf{H}^t$ is the transpose of **H**. The recovery matrix had dimensions 61x3, and was used to compute the recovered radiances from three different sets of computed camera responses, as explained below.

Three additional data sets were used for verification of the method's accuracy. Test set 1 was formed using 30000 randomly selected pixels of the matrix-training set. For this test set, then, we expect the best results, since the radiances included in it were also used to compute the recovery matrix **D**. Test set 2 was formed from 30000 additional pixels of the same scenes used to obtain the matrix-training set, but with none of the pixels in common with those of the matrix training set. And test set 3 was formed by 30000 pixels from other scenes (close-up views of natural scenes not used in the matrix-training set). The recovered spectra were computed as $\mathbf{S}_1$=$\mathbf{D}\mathbf{R}_1$ from the calculated camera responses $\mathbf{R}_1$ to these test sets.

The goodness-of-fit coefficient (GFC), defined as the cosine of the angle between the recovered signal $\mathbf{S_1}$ and original signal **S** in the 61-dimensional space. This commonly used measure of spectral similarity has the advantage of not being affected by scale factors. The other measures were root mean square error (RMSE) and CIELAB color difference ΔE*ab, calculated with reference to the color signal of a white patch included in the scene for illuminant estimation. For spectral reflectances, an equienergy illuminant was assumed for the evaluation of colour differences, since the aim of the work is to compare results obtained with different radiance test sets.

Results and Comment

Figure 1 shows four representative examples of spectral-radiance recovery (two radiances belong to test set 1 and the other two to test set 2). The recovered radiances were computed using the calculated camera responses $\mathbf{R}_1$ for the original radiance spectra and the recovery matrix **D** shown in equation (2). Table 1 shows the mean (and standard deviation) of GFC, RMSE and ΔE^*_{ab} values calculated across all spectral samples (30000) for each test set. The mean GFC value is greater than 0.99 for test set 1. The values of the mean colour differences ΔE^*_{ab}, all less than 1.0, imply that there would be little if any noticeable difference between scene fragments corresponding to recovered and original signals, even with examples such as the one in Fig. 1, top right. This supports the hypothesis that if a visual comparison was made between original and recovered scene fragments, no noticeable differences would be found by a normal colour vision observer.

Table 1. Quality of recovery of spectral radiance from natural scenes with an RGB camera. Mean (SD) over 30000 samples for test sets 1, 2 and 3 are tabulated for three measures of error in spectral recovery.

Test set	GFC
1	0.9920 (0.0057)
2	0.9567 (0.1017)
3	0.9745 (0.0443)
Test set	RMSE
1	0.0015 (0.0013)
2	0.1860 (0.4439)
3	0.0023 (0.0020)
Test set	ΔE^*_{ab}
1	0.3711 (0.1541)
2	0.9112 (0.7859)
3	0.9829 (0.7289)

Recovery was better for test sets 1 and 3 than for test set 2. This was expected, since the recovery matrix was based on test set 1. Test set 3 was less varied than test set 2 and the spectra included in it were probably more similar to those used in the training set, although they corresponded to different scenes and different viewing distances. The results are consistent for the three different quality measures used excepting for ΔE^*_{ab}, whch gives worse recovery quality for test set 3 than for test set 2, while GFC and RMSE give worse recovery quality for test set 2.

Conclusions

Although outdoor natural scenes with uncontrolled illumination present particular problems for recovering radiance spectra, the combination of the direct-mapping method and a commercial RGB digital camera seems to produce satisfactory results, with an average colorimetric error ΔE^*_{ab} of less than unity. These results represent the minimal performance that can be obtained with an RGB camera and may be improved with the introduction of combinations of coloured filters in front of the camera.

These simulations show that a digital RGB camera and a suitable calibration process can produce a spectral capture system with accuracy enough for some applications. Probably tests made with real data would not give results as good as those shown here, due to the presence of noise and problems inherent to spectral measurements in natural environments. Nevertheless, future work include the possibility of checking the accuracy of the recovery process obtained with real camera responses. This could be feasible if some natural scenes were captured with a digital RGB camera and simultaneously pixel-by-pixel spectra for the same scene were measured by a hyoerspectral system such as that described in the Methods section.

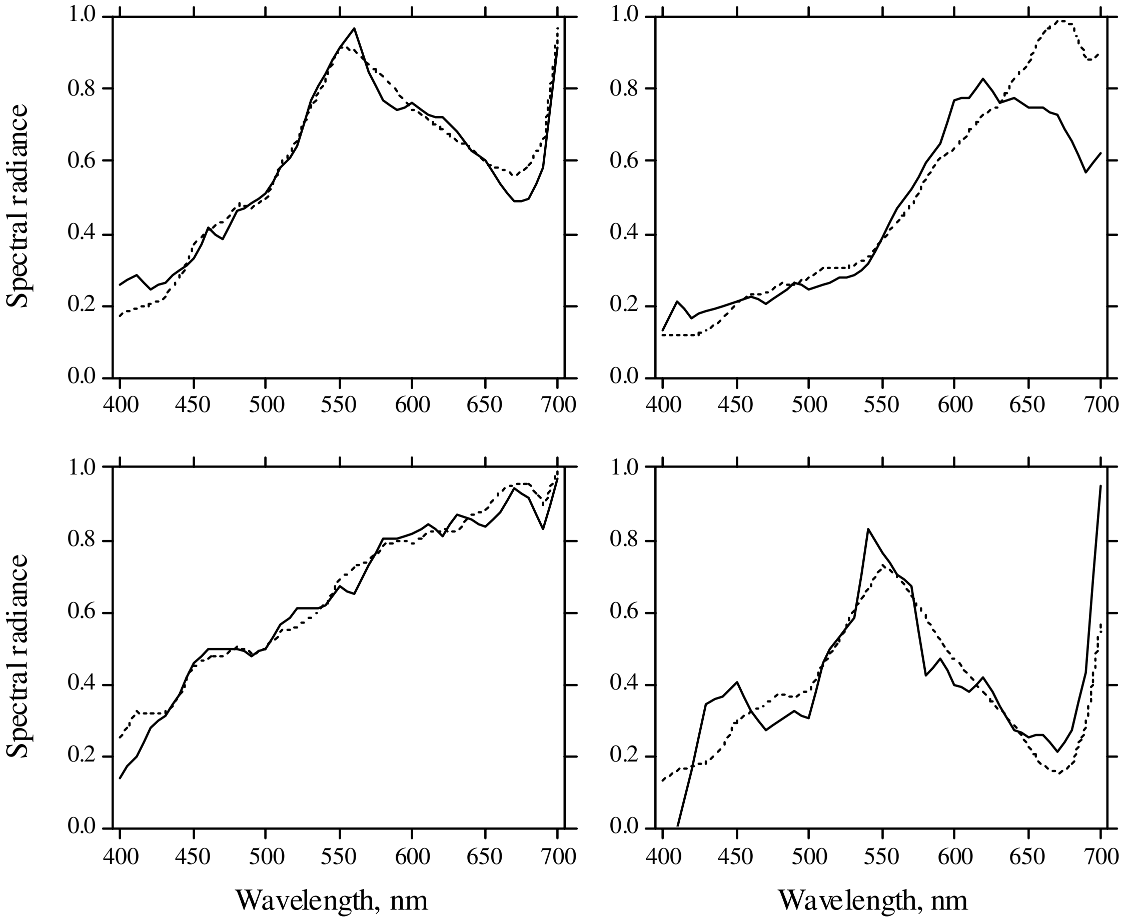

Figure 1. Normalized spectral radiances recovered for two members of test set 1 (upper left GFC = 0.9978, upper right GFC = 0.9795) and two members of test set 2 (lower left GFC = 0.9984, lower right GFC = 0.9505). Original spectra are shown by continuous lines, recovered spectra by broken lines.

References

[1] P.D. Burns and R. S. Berns. Analysis of multispectral image capture. In Proceedings of the IS&T/SID Fourth Color Imaging Conference Color Science, Systems, and Applications, pp. 19-22. Springfield, Va.: Society for Imaging Science and Technology. [2] M. Smith, "Digitial Imaging J. Imaging. Sci. and Technol., 42, 112 (1998).

[2] J. L. Nieves, Valero, E.M., S. M. C. Nascimento, J. HernandezAndres, J. Romero. "Multispectral synthesis of daylight using a commercial digital CCD camera," Applied Optics 44(27), 5696-5703 (2005).

[3] S. M. C. Nascimento, F. P. Ferreira, and D. H. Foster, "Statistics of spatial cone-excitation ratios in natural scenes," Journal of the Optical Society of America A-Optics Image Science and Vision 19(8), 1484-1490 (2002). [2] M. Smith, "Digitial Imaging J. Imaging. Sci. and Technol., 42, 112 (1998).

[4] C. C. Chiao, T. W. Cronin, and D. Osorio, "Color signals in natural scenes: characteristics of reflectance spectra and effects of natural illuminants," Journal of the Optical Society of America A-Optics Image Science and Vision 17(2), 218-224 (2000).

[5] V. Cheung, C. Li, S. Westland, J. Hardeberg, and D. Connah, "Characterization of trichromatic color cameras using a new multispectral imaging technique," Journal of the Optical Society of America A-Optics Image Science and Vision 22(7), 1231-1240 (2005).

[6] J. Romero, A. García-Beltrán, and J. Hernández-Andrés, "Linear bases for representation of natural and artificial illuminants," Journal of the Optical Society of America A-Optics Image Science and Vision 14(5), 1007-1014 (1997).

[7] S. M. C. Nascimento, D.H. Foster, K. Amano, "Psychophysical estimates of the number of spectral-reflectance basis functions needed to reproduce natural scenes," Journal of the Optical Society of America A-Optics Image Science and Vision 22(6), 1017-1022 (2005).

[8] F. H. Imai, L. A. Taplin, D. C. Day, E. A. Day, and R. S. Berns, "Imaging at the National Gallery of Art, Washington D.C.," Technical Report (2002). From http://art-si.org

[9] D. H. Foster, S. M. C. Nascimento, and K. Amano, "Information limits on neural identification of colored surfaces in natural scenes," Visual Neuroscience 21(3), 331-336 (2004).

Author Biography

Dr. Eva M. Valero obtained her Ph.D. by the University of Granada (Spain) in June 2000. Since 1997 she has been a member of the department of Optics, researching in the field of spatial colour vision (recently color image processing) and also teaching since 2001. She has worked in collaboration with the Physiological Laboratory at Cambridge (UK) and the Department of Neurological and Vision Sciences at Verona (Italy)..